Geophysical Research Letters

RESEARCH LETTER

10.1029/2018GL081482

Key Points:

- The largest and most prolonged Maud Rise polynya since the1970s appeared on 14 September 2017 with an areal extent of ~9.3×10^3 km^2
- Record negative anomalies of sea-ice concentration occurred and the polynya expanded up to ~298.1×10^3 km^2 and existed for 79 days
- The polynya was associated with a large cyclonic ocean eddy, negative wind stress curl, and anomalous atmospheric circulation

Supporting Information:

- Supporting Information S1

Correspondence to:
B. Jena,
bjena@ncaor.gov.in

Citation:
Jena, B., Ravichandran, M., & Turner, J. (2019). Recent reoccurrence of large open-ocean polynya on the Maud Rise seamount. *Geophysical Research Letters*, *46*. https://doi.org/10.1029/2018GL081482

Received 28 NOV 2018
Accepted 30 MAR 2019
Accepted article online 5 APR 2019

Recent Reoccurrence of Large Open-Ocean Polynya on the Maud Rise Seamount

B. Jena[1], M. Ravichandran[1], and J. Turner[2]

[1]ESSO-National Centre for Polar and Ocean Research, Ministry of Earth Science, Government of India, Vasco-da-Gama, India, [2]British Antarctic Survey, Natural Environment Research Council, Cambridge, UK

Abstract Satellite observations have shown that the largest and most prolonged Maud Rise open-ocean polynya since the 1970s appeared on 14 September 2017 (~9.3×10^3 km^2) within the seasonal sea-ice cover which expanded maximum on 1 December 2017 (~298.1×10^3 km^2) and existed for 79 days. Record negative anomalies of sea-ice concentration were observed in and around the polynya. The occurrence of the polynya was associated with a large cyclonic eddy and negative wind stress curl that facilitated melting of sea-ice. Concurrently, a region of positive sea level pressure anomalies extended over the entire northern Weddell Sea accompanied by record low negative anomalies (deep depressions) over the southwest Weddell Sea and the Maud Rise. The atmospheric circulation anomalies advected moist-warm air from the midlatitudes, resulted a record atmospheric warming (~11.5 °C) in the Maud Rise that favored this rare event as one of the largest open-ocean polynyas.

Plain Language Summary The polynya plays an important role in the Earth's climate system by modulating the albedo, air-sea exchange of heat, fresh water, carbon, and ocean-atmospheric circulation. The occurrence of such feature is critical for assessing the role of high latitude ocean-atmospheric dynamics in the global climate and also for the Antarctic marine ecosystem. Satellite observations show that a large and most prolonged Maud Rise polynya (Lazarev Sea) reappeared on 14 September 2017 for the first time since its frequent appearance during the 1970s. On 14 September 2017, the areal extent of the polynya was ~9.3×10^3 km^2 which expanded maximum on 1 December 2017 up to ~298.1×10^3 km^2, lasting for 79 days. The formation of the polynya was due to the combined influence of the (i) existence of the geological feature such as a seamount (leads to local upliftment of thermocline), (ii) upwelling of warm water into the upper ocean from the thermocline (induced by a large cyclonic ocean eddy and negative wind stress curl), and (iii) the large-scale anomalous atmospheric warming.

1. Introduction

Open-ocean polynyas are regions of open water within the seasonal sea-ice cover, occurring away from the shore. The occurrence of such polynya is known to have consequence on the Antarctic bottom water properties (Zanowski et al., 2015), atmospheric circulation (Weijer et al., 2017), Antarctic marine ecosystem (Labrousse et al., 2018; Stirling, 1997), carbon uptake, and primary production (Arrigo & van Dijken, 2003; Shadwick et al., 2017). Understanding the interaction between the polynyas and overlaying atmosphere is crucial for assessing the role of high-latitude dynamics in global climate (Maqueda, 2004). The first-ever synoptic observations of a polynya was captured after the launching of Nimbus-5 (Electrically Scanning Microwave Radiometer) in 11 December 1972, which could provide an unprecedented view of the large open-ocean polynya (200–300 × 10^3 km^2) on the Maud Rise (MR) during 1974–1976 (Carsey, 1980; C. De Lavergne et al., 2014). After 1976, polynyas having a similar size and duration have not reappeared on the MR except its recent reappearance in 2017 (Figures 1a, 1b, and S1).

In order to understand the formation mechanism of the MR polynya, theoretical and modeling studies has been linked its occurrence to static instability and open-ocean convection (Martinson et al., 1981; Motoi et al., 1987); Taylor column circulation (Alverson & Owens, 1996; Kurtakoti et al., 2018; Muench et al., 2001); cyclonic ocean eddies and atmospheric processes (de Steur et al., 2007; Holland, 2001); strong wind stress (Cheon et al., 2015); interaction between tidal flow, ocean current, and winds (Beckmann et al., 2001); buildup of the oceanic heat reservoir (Dufour et al., 2017); Southern Annular Mode (SAM) and El Niño-Southern Oscillation (Gordon et al., 2007). Most of these studies suggested that the subsurface warm saline water should reach to the upper ocean for the melting of sea-ice and to form a polynya on the MR.

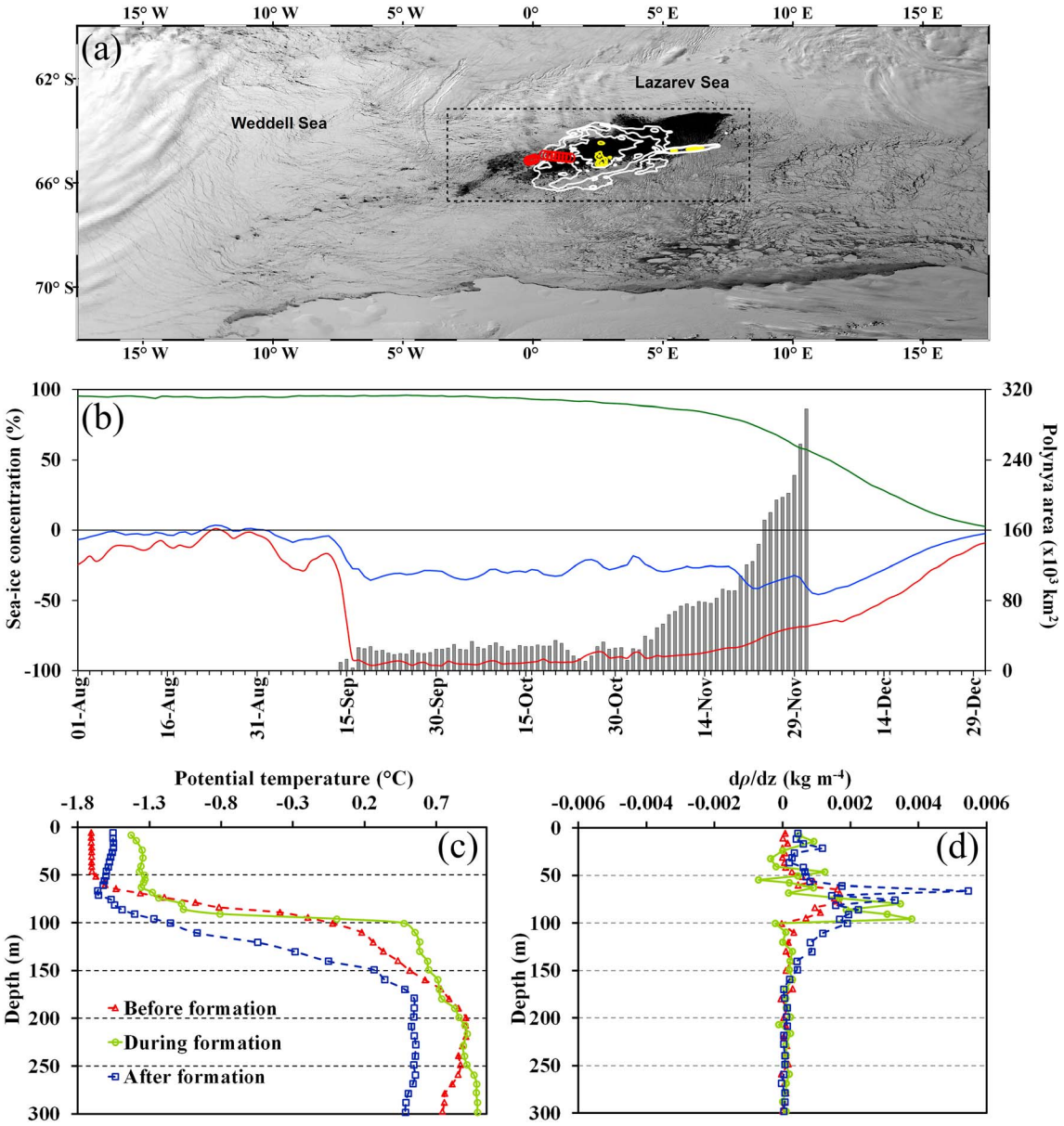

Figure 1. (a) High resolution Aqua-Moderate Resolution Imaging Spectroradiometer image at 859 nm captured an exceptional view of the Maud Rise polynya on 25 September 2017 (1,430 hr UTC). Red circles show the locations of an Argo float from 13 August to 5 December 2017. Yellow lines show the depth contours shallower than 2,000 m and other white contours are spaced by 500 m. (b) The daily changes in mean (blue) and minimum (red) sea-ice concentration anomaly for August–December 2017 relative to the 1979–2016 climatology (green), spatially averaged over the polynya region within the dashed rectangle shown in Figure 1a. Gray bars show the daily areal extent of the polynya. Argo float profiles indicate (c) potential temperature and (d) vertical density gradient for 2017 polynya.

The static instability induced through winter cooling and brine rejection due to sea-ice formation leads to deep convection. The deep convection leads to upwelling of warm circumpolar deep-water from the Weddell Gyre favors for the formation of polynyas (Martinson et al., 1981; Motoi et al., 1987). Also, the oceanic diffusion and entrainment heat fluxes maintains the stability, which can have a positive or negative feedback (Goosse & Zunz, 2014; Hobbs et al., 2016). Cheon et al. (2015) suggested negative wind stress curl over the Weddell Sea (WS) intensifies the cyclonic Weddell Gyre and causes the upwelling of warm-saline deep water to the surface for generating an open-ocean polynya on the MR. The model simulations suggested the influence of synoptic atmospheric variability for the formation of a polynya occurs through transient low-pressure system and divergence of sea-ice (Arbetter et al., 2004; Holland, 2001). The meridional wind advects warm-moist air from the midlatitudes or cold-dry air from the high-

latitudes that affects the melting and growth of sea-ice (Hobbs et al., 2016). Recently, the impact of atmospheric processes resulted in a record decrease in sea-ice during 2016–2017, through enhanced advection of midlatitude warm air into the Antarctica (Ionita et al., 2018; Schlosser et al., 2018; Turner et al., 2017). However, its role for the recent appearance of a large polynya on the MR is not yet examined.

In this article, we show the evidences from satellite data (optical and passive microwave) for the appearance of a large polynya and record loss of sea-ice on the MR during the period from September to December 2017. We reported this rare event with the backdrop of an observed unusual ocean-atmospheric condition on the seamount.

2. Materials and Methods

In order to characterize the MR polynya, we used daily and monthly sea-ice concentration (SIC) data (1979–2017) from multiple passive microwave sensors, such as the Scanning Multichannel Microwave Radiometer, the Special Sensor Microwave Imager, and the Special Sensor Microwave Imager Sounder with spatial resolution of 25 × 25 km acquired from the National Snow and Ice Data Center (Data id-G02135, Version-3). The data were generated using the NASA Team algorithm, which converts satellite-derived brightness temperatures to quality-controlled SIC (Cavalieri et al., 1997; Fetterer et al., 2016). We computed the areal extent of MR polynya by summing-up the total number of pixels (where the SIC is less than or equal to 15%) multiplied with the spatial resolution of a pixel (25 × 25 km; Weijer et al., 2017). The SIC anomalies (both daily and monthly) were computed for the period of August to December 2017 relative to a 38-year climatology (1979–2016). The computation of climatology ignored the missing values for the period from 3 December 1987 to 12 January 1988. The data were available only for alternative days prior to 20 August 1987 and therefore we computed the values for a missing day after averaging between previous and following day values. We used sea-ice drift data from the multiple microwave sensors using a continuous maximum cross correlation method and a multisensor merging strategy (T. Lavergne, 2016). The calibrated radiance values in the infrared-channel (859 nm) from Aqua-Moderate Resolution Imaging Spectroradiometer acquired with the high spatial resolution of ~250 m; however, only few cloud free scenes were available. The bathymetry of the seamount was mapped using Earth Topography One-Arc-Minute Global Relief Model, 2009 (www.ngdc.noaa.gov; Jena et al., 2012) and converted to polyline features with a contour interval of 500 m for showing the seamount extent.

In order to examine the role of ocean processes for the formation of the polynya, we used satellite observations and hydrographic profiles from an Argo float (ID-5904468; Figures 1 and 2). Multimission merged satellite altimeter-derived sea surface height anomalies and geostrophic currents were obtained from AVISO (https://las.aviso.altimetry.fr/) at a resolution of 0.25° × 0.25° (Armitage et al., 2018; Figures 2a–2d). We used Metop-Advanced Scatterometer wind stress curl and Ekman upwelling data distributed by the National Oceanic and Atmospheric Administration (https://coastwatch.pfeg.noaa.gov) at a spatial resolution of 0.25° × 0.25° (Anderson et al., 2011; Pond & Pickard, 1983; Verhoef et al., 2017; Figures 2e–2l). The optimal interpolated sea surface temperature (SST) data (9 × 9 km) obtained from Remote Sensing Systems (www.remss.com), which was produced after merging of the microwave and infrared SSTs using an optimal interpolated scheme (Reynolds & Smith, 1994; Figures 2m–2p). We used profiles from an Argo float that had remained in the polynya from August to December 2017 (http://www.argo.ucsd.edu/). To bring out the persistent features, we have averaged the spatial profiles corresponding to the periods before (13 August to 3 September 2017) and after (24 September to 5 December 2017) the polynya formation (Figures 1c and 1d and S2a and S2b). The profile available on 13 September was considered as the reference day of its formation even though the event had occurred just after 1 day. We calculated vertical density gradient ($d\rho/dz$) to interpret the static stability. The mixed layer was calculated as the uppermost layer of uniform potential density with the depth at which the value in the upper layer varies by 0.01 kg/m^3 reference to the surface (Figure S2b; Kaufman et al., 2014). The quality-controlled monthly potential temperature (1979–2017) data were examined using the European Centre for Medium-Range Weather Forecast (ECMWF)'s advanced operational ocean reanalysis system (ORAS4; Figures S2c–S2f and S3a; Balmaseda et al., 2013) and the Copernicus Marine Environment Monitoring Service (Figure S3b–S3e).

The role of atmospheric circulation anomalies for the formation of MR polynya was examined using the ECMWF's Interim (ERA-Interim) daily and monthly reanalysis fields, available at 0.25° × 0.25° grid

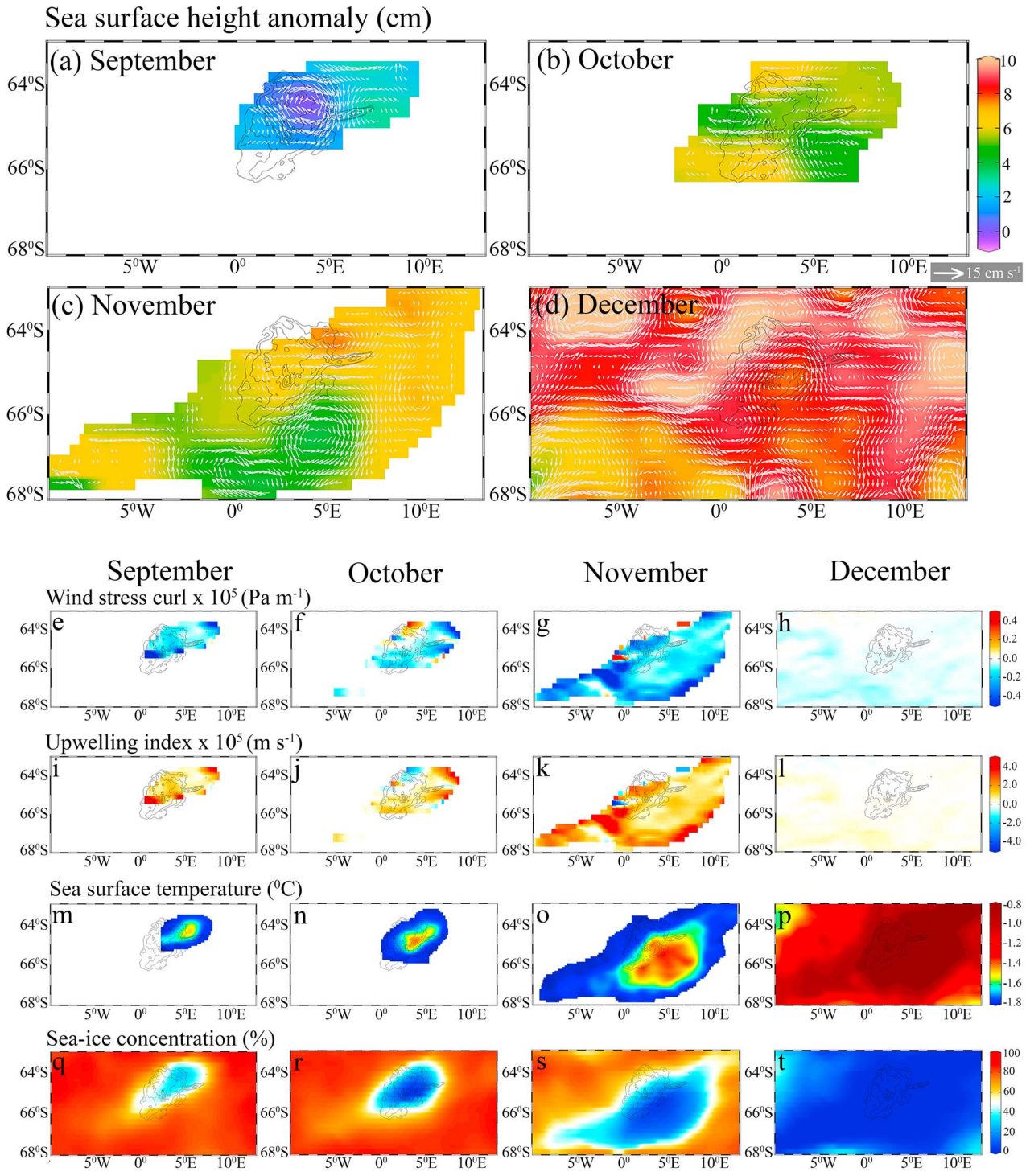

Figure 2. Monthly mean of (a–d) sea surface height anomaly and geostrophic current velocity (white arrows), (e–h) wind stress curl, (i–l) upwelling index, (m–p) sea surface temperature, and (q–t) sea-ice concentration during the period of polynya occurrence from September to December 2017.

(www.ecmwf.int). We used SAM index (Marshall, 2003) available online (at https://legacy.bas.ac.uk/met/gjma/sam.html). Although this article has focused mainly on the event during 2017, we additionally analyzed the ocean-atmospheric data for the polynya occurred in 2016 for comparing the mechanism of formation.

3. Results and Discussion

3.1. Satellite Observation of Polynya Formation

Analysis of Special Sensor Microwave Imager Sounder daily maps show that a region of low SIC (~48%) developed within the seasonal sea-ice cover on the north-east flank of MR seamount on 2 September 2017 (Figure not shown). It further reduced up to ~36% until 13 September (Figure S1p). Subsequently, a polynya with areal extent of ~9.3×10^3 km^2 developed on 14 September 2017, approximately at 4.7°E and 64.4°S (Figure S1q). High-resolution Aqua-Moderate Resolution Imaging Spectroradiometer radiance data on 25 September 2017 captured an exceptional view of the polynya and its surrounding features of broken sea-ice (Figure 1a). The polynya expanded maximum to a large opening of ~298.1×10^3 km^2 on 1 December 2017 and lasted for 79 days (Figures 1b and S1r). The areal coverage was nearly static during September–October 2017, however it rapidly enlarged and shifted 169 km southeastward during November 2017 (Figures 1b and 2q–2t). On 2 December 2017, a very low SIC (~12%) developed at the north-eastern edge (~10.51°E, 62.28°S) with a length of 25 km (East–West) and 52 km (North–South) that had separated the polynya from the open-ocean (Figure S1s). On 3 December 2017, the SIC reduced (~9%) in this edge with an enhanced length of 145 km (East–West) and 52 km (North–South). Its northern boundary was completely disappeared by 10 December 2017, in the proximity of a warmer sea surface to the north. Spatially averaged daily SIC within the MR (3.28°W to 8.32°E and 66.7 to 63.14°S) indicated a climatological value of 90% persisted during 1 August to 8 October, however, a gradual decline follows in the start of the melt season (Figure 1b). The daily mean and minimum values of the SIC anomaly indicated a consistent negative anomaly that started on 14 September and continued till 31 December 2017. Satellite observations shown that the event observed in September–December 2017 was the largest and most prolonged open-ocean polynya on the MR since its appearance during 1974–76, except occasional opening during September 1994, August 2016, November–December 2016, and June 2017. We describe the role of both ocean and atmospheric processes to explain the occurrence of MR polynya in September through December 2017.

3.2. Oceanic Influence

Analysis of bathymetry showed that the top of the MR seamount is located at 2.63°E and 65.23°S, which rises from the abyssal plain of ~5,200 m to the shallowest depth of ~968 m (Figure S4a). Local upliftment of thermocline occurs in presence of a seamount (Muench et al., 2001; Roden, 2013). The climatological profiles of potential temperature in September (1979–2016) shows the thermocline is uplifted about 22 m due to the presence of seamount (Figure S3a). The water column on the seamount is characterized by the presence of a cold-fresh layer in the upper ocean separated from a lower warm-saline layer by a weak pycnocline (de Steur et al., 2007; Figures 1c, S2a, and S2b). The water column has a low static stability (Figure 1d) that favors convection and mixing in turn that brings warm-saline water from the thermocline to the upper ocean (Goosse & Zunz, 2014; Gordon & Comiso, 1988; Lefebvre et al., 2004; Martinson et al., 1981; Muench et al., 2001), leading to usual low SIC on the MR seamount (Figure S5). Therefore, the oceanic processes that can bring warm water into the upper ocean from the thermocline have an important role for melting of sea-ice and formation of polynya. In order to identify the oceanic process that can cause the appearance of a polynya, we examined oceanographic data during September–December 2017 and the results are shown in Figure 2.

Analysis of monthly sea surface height anomalies and corresponding geostrophic currents indicated the presence of a large cyclonic eddy having a diameter of ~220 km in the vicinity of MR seamount during September 2017 (Figure 2a). The center of the cyclonic eddy was approximately located at 3.84°E and 64.47°S, closely matching with the center of the polynya having warm SST (−1.35 °C) compared to its peripheral cold SST of −1.79 °C (Figures 2a and 2m). The influence of this cyclonic eddy to form a polynya on the MR has two different roles. Primarily, the eddy brings the warm thermocline water into the sea surface through Ekman upwelling that results in a pool of warm SST at its center and facilitated the melting of sea-ice for the opening of polynya in September (Figure 2). Additionally, the eddy transmits divergence on the sea-ice cover that can enhance the open water fraction and gains access to the atmosphere (Holland, 2001). A cyclonic flow pattern of sea-ice was observed (indicating a divergence) with an overall southwesterly strong drift during September (Figure S4b). The polynya extent was nearly static from September to October, and shifted southward during November in conjunction with the southward movement of cyclonic eddy accompanied by a pool of warm SST (Figure 2). Although a dipole structure of cyclonic and

anticyclonic eddies was observed on the MR, a large cyclonic eddy dominated the flow pattern (Figures 2a–2d). The shape and movement of the cyclonic eddy matching well with the movement of the annular pattern of the polynya and annular halo of warm SST (Figure 2). The transient nature and appearance of such events are theoretically attributed to the transient nature of ocean current interaction with the MR that spawns a large cyclonic eddy off the northeast flank of the seamount (Holland, 2001).

The interaction between the ocean current and the MR seamount is known to trigger various dynamic features which have an important role for the formation of a polynya. An isolated water column (Taylor column) trapped over the MR seamount hinders the horizontal flow over the rise and intensifies the flow around its periphery (Alverson & Owens, 1996; Ou, 1991). This causes a ring-shaped closed circulation and a warm pool over the MR which has been considered as the dynamical necessary region of cyclonic vorticity associated with a Taylor column (Muench et al., 2001). Various warm cores and sharp fronts were associated with this closed circulation pattern (Bersch et al., 1992; Gordon & Huber, 1990), along with an eddy dipole on the MR (Muench et al., 2001). Also, the sea-ice-ocean model simulations demonstrated the interaction between ocean current and the MR seamount spawns a cyclonic eddy that enhances the open water fraction within the sea-ice cover (de Steur et al., 2007; Holland, 2001; Ou & Gordon, 1986), and the phenomenon confirms the validity of our observations (Figures 2a–2d). We also find that the sea surface on the MR seamount was forced by negative wind stress curl (Figures 2e–2h), favorable for the upwelling of subsurface warm water to the surface (Figures 2i–2l). Wind stress supports for the opening of polynya through Ekman upwelling and triggering the formation of convection cells (Gordon & Huber, 1990). The resulted upwelling of deep warm water plays an important precondition for the occurrence of a long-lived and large-scale open-ocean polynya on the MR (Cheon et al., 2015).

In addition to satellite observations, we have analyzed profiles from an Argo float (ID-5904468). Before the formation of polynya (13 August to 3 September 2017), the hydrographic profile up to 300 m depth indicate an average mixed layer of ~60 m having relatively cold (−1.69 °C) and low saline (34.52 psu) water mass separated from a lower warm (up to 0.89 °C) and saline (up to 34.76 psu) water mass (Figures 1c, S2a, and S2b). During the formation of the polynya, the mixed layer deepened to ~73 m on 13 September with average temperature (salinity) of −1.34 °C (34.50 psu). The observed mixed layer increase of ~13 m and warming of 0.35 °C as shown in Argo data, also evident in SSTs derived from satellite measurements (Figures 2m–2p). Depth-Latitude cross section of ORAS4 potential temperature data at 4.7°E and 64.5°S suggested that anomalously deep warm water was ventilated and brought closer to the upper ocean from the thermocline (upward doming of isotherms) that could facilitate for melting of sea-ice during September–December 2017 (Figures S2c–S2f). A high-resolution (1/12°) eddy-resolving model data from the Copernicus Marine Environment Monitoring Service indicated that subsurface warm water is uplifted from the thermocline along 4.7°E (Figures S3b–S3e). The presence of the polynya was consistent with the areas of anomalously warm sea surface and subsurface temperature (Figures 2m–2t and S2c–S2f).

While favorable oceanic circulation (cyclonic eddies) and wind stress curl had important roles for the opening of the polynya through upwelling processes, it has been suggested that both oceanic and atmospheric processes should take place concurrently on different scales in order to provide the conducive environment for a large polynya to form (Arbetter et al., 2004; de Steur et al., 2007).

3.3. Atmospheric Influence

In order to study the influence of synoptic atmospheric variability on the MR sea-ice, we examined ECMWF reanalysis data (1979–2017) and the results are shown in Figure 3. During August 2017, a center of positive mean sea level pressure (SLP) anomaly occurred in the central WS and south-west WS, accompanied by negative anomalies over the MR and zone of 60–65°S (Figure 3a). This SLP pattern directed south-easterly wind into the southern region of the MR and westerly wind into the northern region of the MR. No anomalous features of SIC observed in the vicinity of MR during August.

During September 2017, the atmospheric circulation indeed changed dramatically. A region of positive SLP anomalies extended over the entire northern WS, accompanied by a record low negative anomaly (a deep depression) over the southwest WS and the MR (Figure 3b). The SLP over the southwest WS in September 2017 was the lowest recorded value relative to September 1979–2016 (968 hPa compared to climatological mean of 986 hPa). The areas within thick polyline shown the record level anomalies in September 2017

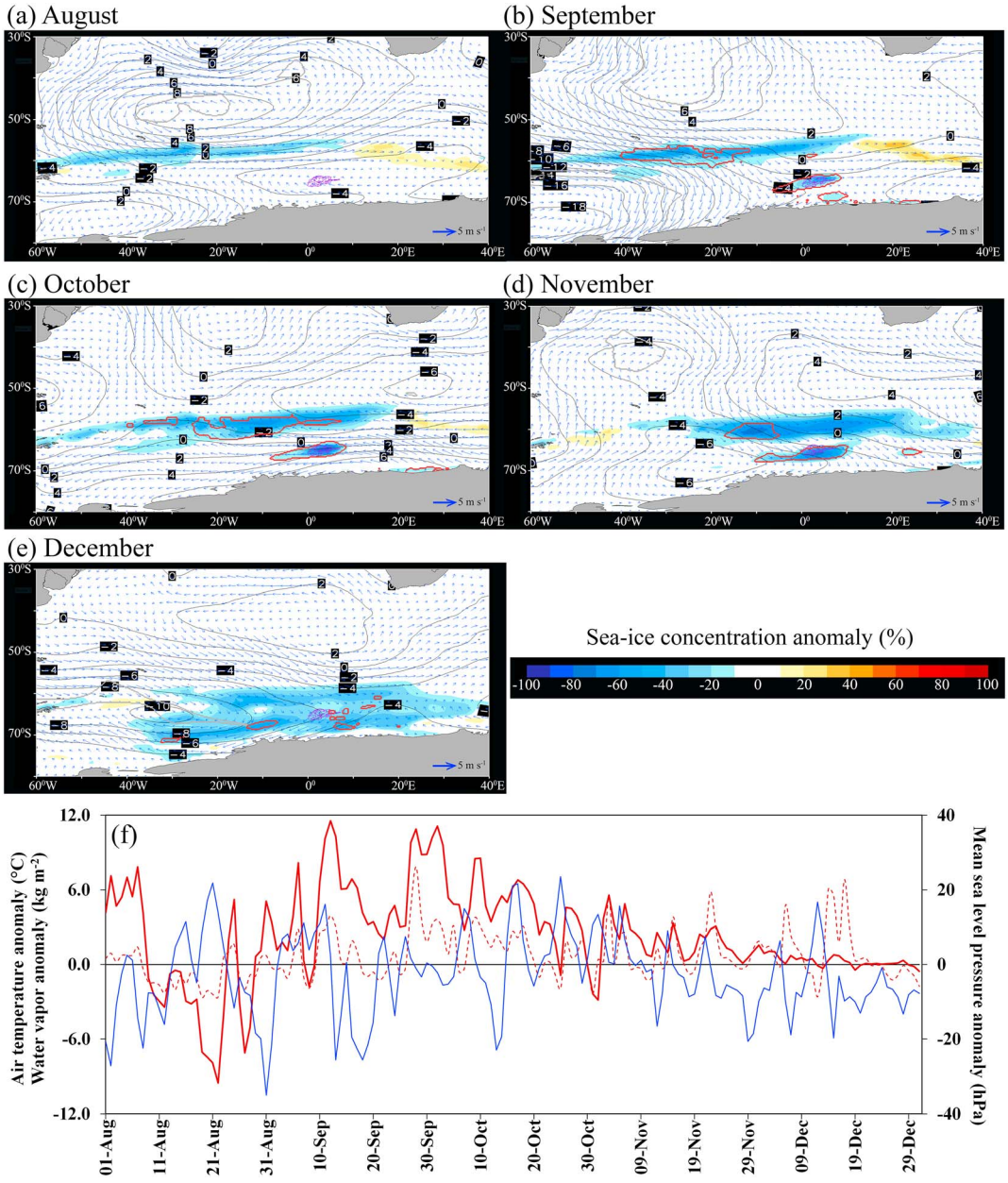

Figure 3. Monthly anomalies of mean sea level pressure (SLP, gray contours) and 10-m wind vector overlaid on anomalous sea-ice concentration (SIC) for 2017 (a) August, (b) September, (c) October, (d) November, and (e) December. The regions within red (gray) thick polylines shows the record level SIC (SLP) in 2017 that lies outside of SIC (SLP) values from 1979 to 2016. Purple polylines showing the depth contours of Maud Rise seamount. (f) Daily changes in 2-m air temperature (red), integrated water vapor (dashed), and SLP (blue) anomalies for September–December 2017 relative to a 38-year climatology (1979–2016), spatially averaged over the polynya region within the dashed rectangle shown in Figure 1a.

relative to September 1979–2016. The observed depression directed strong north-westerly flow of anomalously warm and moist air from the midlatitudes into the MR through the marginal ice zone (MIZ), with a marked meridional pattern (Figures 3b, S6a, and S7a). Correspondingly, anomalous high air temperature (AT; ~6 °C) and vertical integrated water vapor (~2 kg/m^2) was observed on the MR and also along the flow direction (Figures S6a and S7a). Analysis of daily maps indicated large negative SIC anomalies occurred corresponding to repetitive episodes of deep depressions over the southwest WS, that advected warm and moist air into the MR, with strong episodes occurred during 11–18, September 2017 (Figure not shown). Spatially averaged (3.28°W to 8.32°E and 66.7 to 63.14°S) daily net heat flux over the

MR indicated a positive anomaly up to ~57 W/m^2 before the formation of polynya (Figure S8). A large positive anomaly of AT (~11.5 °C), integrated water vapor (~3.9 kg/m^2), and SLP (25.5 hPa) were observed in prior to the formation of polynya during 12 September (Figure 3f). The peaks in AT associated with drop in SLP are, respectively, the signature of the fronts and the passage of cyclones (Francis et al., 2018). The strong north-westerly flow of anomalously warm and moist air into the MR contributed to the observed record low SIC and likely to the formation of the polynya (Figure 3b). Such anomalous atmospheric circulations have been noticed to have significant impacts on Antarctic sea-ice loss (Doddridge & Marshall, 2017; Ionita et al., 2018; Schlosser et al., 2018; Turner et al., 2017), however, are more pronounced on the MR and the MIZ (Figure 3b) due to its climatological low SIC (Figure S5). The appearance of the polynya and anomalously negative SIC was associated with the SLP pattern similar to a positive phase of SAM (index of 0.42). However, the SLP pattern was not annular due to the presence of deep depressions in the southwest WS (Figure 3b). Lefebvre et al. (2004) noted that the nonannular component of the SLP pattern associated with a positive SAM leads to enhanced meridional flow of warm air from the midlatitudes into the WS that contributes to the melting of sea-ice, in addition to the contribution from strong upwelling of warm water. During the negative SAM, sea-ice cover was increased over the WS with colder air brought in with the enhanced northward wind (Gupta & England, 2006).

During October, the polynya extent did not change a great deal (Figures 1b, 2q, and 2r) corresponding to a negative SAM pattern (−0.64) accompanied by anomalously high SLP over the MR and coastal Antarctica and low SLP to its north, that drove cold easterly flow into the MR (Figure 3c). The polynya expanded rapidly in November (Figures 1b and 2s) associated with anomalously low SLP (a couple of depressions at 20°W, 67.5°S and 35°W, 44°S) in the western WS and high SLP in the Lazarev Sea (Figure 3d) corresponding to a strong positive phase of SAM (index of 3.18). The east-to-west SLP anomaly directed meridional flow of north-westerly warm and moist air from the midlatitudes into the MR that contributed for rapid expansion of the polynya. Persistent positive anomalies of NHF reached up to ~140 W/m^2 during the rapid expansion in November (Figure S8). During December, the polynya completely disappeared and the entire WS and Lazarev Sea experienced anomalously negative SIC except in the part of southwest WS (Figure 3e). The SLP variability followed a positive SAM pattern in December (index of 1.44) and there was a deep depression (at 32°W, 65°S) with a negative SLP anomalies (976 hPa compared to climatological mean of 987 hPa) observed over the southwest WS. The anomalous northwesterly flow of warm and moist air into the MR facilitated for the anomalous negative SIC in December 2017.

We have also analyzed the events in 2016 (Figures S9 and S10). The small polynya occurred during August 2016 was associated with an anomalous pattern of negative SLP (up to ~8 hPa) with a cyclonic wind pattern on the MR (Figure S10a) that directed strong north-westerly flow of anomalously warm air from the midlatitudes. Anomalously high AT up to ~6 °C was observed on the MR accompanied with the negative SIC anomalies (Figure S10b). The presence of mobile depressions that moved from the Bellingshausen and Amundsen Seas into the southern WS was responsible for such changes in SIC (Turner et al., 2017). Although the atmospheric condition was favorable for the formation of polynya; however, the oceanic influence should have a major role for the initiation. Analysis of an event during November 2016 revealed the presence of two cyclonic ocean eddies (located at 6.0°E, 66.77°S and 0.10°E, 67.72°S) and favorable pattern of negative wind stress curl leads to upwelling of subsurface warm water to the upper ocean; in turn could facilitate for the melting of sea-ice (Figure S9).

4. Summary and Conclusion

We have shown that the largest and most prolonged MR open-ocean polynya since the 1970s reappeared on 14 September 2017 and lasted for 79 days. Record negative anomalies of SIC were observed on the MR from September to December 2017. We described anomalous ocean-atmospheric conditions which facilitated the formation of this rare event. The occurrence was primarily associated with a large cyclonic eddy and upward doming of isotherms over the MR seamount in September 2017. The center of the polynya shifted southward in conjunction with a cyclonic eddy movement and pools of anomalously warm SST. The eddy brought relatively warm subsurface water from the thermocline to the upper ocean that facilitated melting of sea-ice. Also, the MR sea surface was forced by favorable wind stress curl for upwelling of subsurface warm water. Concurrently, the atmospheric circulation anomalies associated with depressions in the southwest WS

ensued enhanced advection of warm-moist air from midlatitudes into the MR with a marked meridional pattern, giving rise to a record high atmospheric temperature and decrease in SIC. The decrease in SIC was pronounced only on the MR and the MIZ of the WS, due to its climatologically low SIC.

The past occurrence of polynyas on the MR was attributed to the presence of ocean eddies formed from the interaction between the ocean current and the MR seamount (de Steur et al., 2007; Holland, 2001; Ou & Gordon, 1986). The recent episodic events of record loss in Antarctic sea-ice during 2016 and 2017 was linked to the anomalous atmospheric circulations (Doddridge & Marshall, 2017; Ionita et al., 2018; Schlosser et al., 2018; Turner et al., 2017). With support from earlier findings, we suggest that the polynya was formed due to the combined influence of the MR seamount (leads to local upliftment of thermocline), upwelling of warm water into the upper ocean from the thermocline (induced by a large cyclonic eddy and negative wind stress curl), and the large-scale atmospheric circulation anomalies associated with depressions that advected warm-moist air from the midlatitudes to the MR region. The mechanism of polynya formation in 2016 was similar to that of 2017. Regional atmosphere-ocean-ice modeling is required to quantify the contribution of ocean and atmospheric influences. Also, this will help to understand the impact of such open-ocean polynya on the Southern Ocean and atmospheric circulation using various sensitivity studies.

Acknowledgments

Authors are thankful to A. J. Luis and M. Thamban of NCAOR for their encouragement and support. The authors greatly acknowledge various organizations such as National Snow and Ice Data Center (NSIDC), National Oceanic and Atmospheric Administration (NOAA), European Centre for Medium Range Weather Forecast (ECMWF), National Aeronautics and Space Administration (NASA), Asia-Pacific Data Research Center (APDRC), European Organization for the Exploitation of Meteorological Satellites (EUMETSAT), Copernicus Marine Environment Monitoring Service (CMEMS), and their data processing teams for making various data sets available in their portals. Argo data were available from the Southern Ocean Carbon and Climate Observations and Modeling (SOCCOM) Project funded by the National Science Foundation, Division of Polar Programs (NSF PLR -1425989), supplemented by NASA, and by the International Argo Program and the NOAA programs (http://www.argo.ucsd.edu, http://argo.jcommops.org). The authors would like to thank the anonymous reviewers for their insightful comments and suggestions that have contributed to improve this article. This is NCPOR contribution number 92/2018

References

Alverson, K., & Owens, W. B. (1996). Topographic preconditioning of open-ocean deep convection. *Journal of Physical Oceanography*, *26*(10), 2196–2213. https://doi.org/10.1175/1520-0485(1996)026<2196:TPOOOD>2.0.CO;2

Anderson, C., Figa, J., Bonekamp, H., Wilson, J. J. W., Verspeek, J., Stoffelen, A., & Portabella, M. (2011). Validation of backscatter measurements from the Advanced Scatterometer on MetOp-A. *Journal of Atmospheric and Oceanic Technology*, *29*(1), 77–88. https://doi.org/10.1175/JTECH-D-11-00020.1

Arbetter, T. E., Lynch, A. H., & Bailey, D. A. (2004). Relationship between synoptic forcing and polynya formation in the Cosmonaut Sea: 1. Polynya climatology. *Journal of Geophysical Research*, *109*, C04022. https://doi.org/10.1029/2003JC001837

Armitage, T. W. K., Kwok, R., Thompson, A. F., & Cunningham, G. (2018). Dynamic topography and sea level anomalies of the Southern Ocean: Variability and teleconnections. *Journal of Geophysical Research: Oceans*, *123*, 613–630. https://doi.org/10.1002/2017JC013534

Arrigo, K. R., & van Dijken, G. L. (2003). Phytoplankton dynamics within 37 Antarctic coastal polynya systems. *Journal of Geophysical Research*, *108*(C8), 3271. https://doi.org/10.1029/2002JC001739

Balmaseda, M. A., Mogensen, K., & Weaver, A. T. (2013). Evaluation of the ECMWF ocean reanalysis system ORAS4. *Quarterly Journal of the Royal Meteorological Society*, *139*(674), 1132–1161. https://doi.org/10.1002/qj.2063

Beckmann, A., Timmermann, R., Pereira, A. F., & Mohn, C. (2001). The effect of flow at Maud Rise on the sea-ice cover—Numerical experiments. *Ocean Dynamics*, *52*(1), 0011–0025. https://doi.org/10.1007/s10236-001-8173-5

Bersch, M., Becker, G. A., Frey, H., & Koltermann, K. P. (1992). Topographic effects of the Maud Rise on the stratification and circulation of the Weddell Gyre. *Deep Sea Research Part A, Oceanographic Research Papers*, *39*(2), 303–331. https://doi.org/10.1016/0198-0149(92)90111-6

Carsey, F. D. (1980). Microwave observation of the Weddell polynya. *Monthly Weather Review.*, *108*(12), 2032–2044. https://doi.org/10.1175/1520-0493(1980)108<2032:MOOTWP>2.0.CO;2

Cavalieri, D. J., C. L. Parkinson, P. Gloersen, and H. J. Zwally. (1997). Arctic and Antarctic sea ice concentrations from multichannel passive-microwave satellite data sets: October 1978–September 1995—User's guide. NASA TM 104647. Greenbelt, MD 20771.

Cheon, W. G., Lee, S. K., Gordon, A. L., Liu, Y., Cho, C. B., & Park, J. J. (2015). Replicating the 1970s' Weddell polynya using a coupled ocean-sea ice model with reanalysis surface flux fields. *Geophysical Research Letters*, *42*, 5411–5418. https://doi.org/10.1002/2015GL064364

De Lavergne, C., Palter, J. B., Galbraith, E. D., Bernardello, R., & Marinov, I. (2014). Cessation of deep convection in the open Southern Ocean under anthropogenic climate change. *Nature Climate Change*, *4*(4), 278–282. https://doi.org/10.1038/nclimate2132

de Steur, L., Holland, D. M., Muench, R. D., & McPhee, M. G. (2007). The warm-water "Halo" around Maud rise: Properties, dynamics and impact. *Deep-Sea Research Part I: Oceanographic Research Papers*, *54*(6), 871–896. https://doi.org/10.1016/j.dsr.2007.03.009

Doddridge, E. W., & Marshall, J. (2017). Modulation of the seasonal cycle of Antarctic sea ice extent related to the southern annular mode. *Geophysical Research Letters*, *44*, 9761–9768. https://doi.org/10.1002/2017GL074319

Dufour, C. O., Morrison, A. K., Griffies, S. M., Frenger, I., Zanowski, H., & Winton, M. (2017). Preconditioning of the Weddell Sea polynya by the ocean mesoscale and dense water overflows. *Journal of Climate*, *30*(19), 7719–7737. https://doi.org/10.1175/JCLI-D-16-0586.1

Fetterer, F., Knowles, K., Meier, W., & Savoie, M. (2016). *Sea ice index, version 2 (updated daily)*. Boulder, CO NSIDC: National Snow and Ice Data Center. https://doi.org/10.7265/N5736NV7

Francis, D., Eayrs, C., Cuesta, J., & Holland, D. (2018). Polar cyclones at the origin of the reoccurrence of the Maud Rise polynya in austral winter 2017. *Journal of Geophysical Research: Atmospheres*. https://doi.org/10.1029/2018JD029458R

Goosse, H., & Zunz, V. (2014). Decadal trends in the Antarctic sea ice extent ultimately controlled by ice-ocean feedback. *The Cryosphere*, *8*(2), 453–470. https://doi.org/10.5194/tc-8-453-2014

Gordon, A. L., & Comiso, J. C. (1988). Polynyas in the Southern Ocean the global heat engine that couples the ocean and the atmosphere. *Scientific American*, *258*(6), 90–97. https://doi.org/10.1038/scientificamerican0688-90

Gordon, A. L., & Huber, B. A. (1990). Southern Ocean winter mixed layer. *Journal of Geophysical Research*, *95*(C7), 11,655. https://doi.org/10.1029/JC095iC07p11655

Gordon, A. L., Visbeck, M., & Comiso, J. C. (2007). A possible link between the Weddell polynya and the southern annular mode. *Journal of Climate*, *20*(11), 2558–2571. https://doi.org/10.1175/JCLI4046.1

Gupta, A. S., & England, M. H. (2006). Coupled ocean-atmosphere-ice response to variations in the southern annular mode. *Journal of Climate*, *19*(18), 4457–4486. https://doi.org/10.1175/JCLI3843.1

Hobbs, W. R., Massom, R., Stammerjohn, S., Reid, P., Williams, G., & Meier, W. (2016). A review of recent changes in Southern Ocean sea ice, their drivers and forcings. *Global and Planetary Change*, *143*, 228–250. https://doi.org/10.1016/j.gloplacha.2016.06.008

Holland, D. M. (2001). Explaining the Weddell polynya—A large ocean eddy shed at Maud Rise. *Science*, *292*(5522), 1697–1700. https://doi.org/10.1126/science.1059322

Ionita, M., Scholz, P., Grosfeld, K., & Treffeisen, R. (2018). Moisture transport and Antarctic sea ice: Austral spring 2016 event. *Earth System Dynamics*, *9*(3), 939–954. https://doi.org/10.5194/esd-9-939-2018

Jena, B., Kurian, P. J., Swain, D., Tyagi, A., & Ravindra, R. (2012). Prediction of bathymetry from satellite altimeter based gravity in the Arabian Sea: Mapping of two unnamed deep seamounts. *International Journal of Applied Earth Observation and Geoinformation*, *16*(1), 1–4. https://doi.org/10.1016/j.jag.2011.11.008

Kaufman, D. E., Friedrichs, M. A. M., Smith, W. O., Queste, B. Y., Heywood, K. J., & Sea, R. (2014). Deep-sea research I: Biogeochemical variability in the southern Ross Sea as observed by a glider deployment. *Deep-Sea Research Part I*, *92*, 93–106. https://doi.org/10.1016/j.dsr.2014.06.011

Kurtakoti, P., Veneziani, M., Stössel, A., & Weijer, W. (2018). Preconditioning and formation of Maud rise polynyas in a high-resolution Earth system model. *Journal of Climate*, *31*(23), 9659–9678. https://doi.org/10.1175/JCLI-D-18-0392.1

Labrousse, S., Williams, G., Tamura, T., Bestley, S., Sallée, J.-B., Fraser, A. D., et al. (2018). Coastal polynyas: Winter oases for subadult southern elephant seals in East Antarctica. *Scientific Reports*, *8*(1), 3183. https://doi.org/10.1038/s41598-018-21388-9

Lavergne, T. (2016). Algorithm theoretical basis document for OSI SAF medium resolution sea ice drift product, (May), Version 1.3.

Lefebvre, W., Goosse, H., Timmermann, R., & Fichefet, T. (2004). Influence of the southern annular mode on the sea ice–ocean system. *Journal of Geophysical Research*, *109*, C090005. https://doi.org/10.1029/2004JC002403

Maqueda, M. A. M (2004). Polynya dynamics: A review of observations and modeling, (2002). https://doi.org/10.1029/2002RG000116.1. INTRODUCTION

Marshall, G. J. (2003). Trends in the southern annular mode from observations and reanalyses. *Journal of Climate*, *16*(24), 4134–4143. https://doi.org/10.1175/1520-0442(2003)016<4134:TITSAM>2.0.CO;2

Martinson, D. G., Killworth, P. D., & Gordon, A. L. (1981). A convective model for the Weddell polynya. *Journal of Physical Oceanography*, *11*(4), 466–488. https://doi.org/10.1175/1520-0485(1981)011<0466:ACMFTW>2.0.CO;2

Motoi, T., Ono, N. B., & Wakatsuchi, M. (1987). A mechanism for the formation of the Weddell polynya in 1974. *Journal of Physical Oceanography.*, *17*(12), 2241–2247. https://doi.org/10.1175/1520-0485(1987)017<2241:AMFTFO>2.0.CO;2

Muench, R. D., Morison, J. H., Padman, L., Martinson, D., Schlosser, P., Huber, B., & Hohmann, R. (2001). Maud Rise revisited. *Journal of Geophysical Research*, *106*(C2), 2423–2440. https://doi.org/10.1029/2000JC000531

Ou, H. W. (1991). Some effects of a seamount on oceanic flows. *Journal of Physical Oceanography*, *21*(12), 1835–1845. https://doi.org/10.1175/1520-0485(1991)021<1835:seoaso>2.0.co;2

Ou, H. W., & Gordon, A. L. (1986). Spin-down of baroclinic eddies under sea ice. *Journal of Geophysical Research*, *91*(C6), 7623. https://doi.org/10.1029/JC091iC06p07623

Pond, S., & Pickard, G. L. (1983). *Introductory dynamical oceanography* (2nd ed.). Oxford UK: Butterworh- Heinemann Ltd.

Reynolds, R. W., & Smith, T. M. (1994). Improved global sea surface temperature analyses using optimum interpolation. *Journal of Climate*, *7*(6), 929–948. https://doi.org/10.1175/1520-0442(1994)007<0929:IGSSTA>2.0.CO;2

Roden, G. I. (2013). Effect of seamounts and seamount chains on ocean circulation and thermohaline structure. In *Seamounts, islands, and atolls* (pp. 335–354). Washington, DC: American Geophysical Union. https://doi.org/10.1029/GM043p0335

Schlosser, E., Alexander Haumann, F., & Raphael, M. N. (2018). Atmospheric influences on the anomalous 2016 Antarctic sea ice decay. *The Cryosphere*, *12*(3), 1103–1119. https://doi.org/10.5194/tc-12-1103-2018

Shadwick, E. H., Tilbrook, B., & Currie, K. I. (2017). Late-summer biogeochemistry in the Mertz polynya: East Antarctica. *Journal of Geophysical Research: Oceans*, *122*, 7380–7394. https://doi.org/10.1002/2017JC013015

Stirling, I. (1997). The importance of polynas, ice edges, and leads to marine mammals and birds. *Journal of Marine Systems*, *10*(1–4), 9–21. https://doi.org/10.1016/S0924-7963(96)00054-1

Turner, J., Phillips, T., Marshall, G. J., Hosking, J. S., Pope, J. O., Bracegirdle, T. J., & Deb, P. (2017). Unprecedented springtime retreat of Antarctic sea ice in 2016. *Geophysical Research Letters*, *44*, 6868–6875. https://doi.org/10.1002/2017GL073656

Verhoef, A., Vogelzang, J., Verspeek, J., & Stoffelen, A. (2017). Long-term scatterometer wind climate data records. *IEEE Journal of Selected Topics in Applied Earth Observations and Remote Sensing*, *10*(5), 2186–2194. https://doi.org/10.1109/JSTARS.2016.2615873

Weijer, W., Veneziani, M., Stössel, A., Hecht, M. W., Jeffery, N., Jonko, A., et al. (2017). Local atmospheric response to an open-ocean polynya in a high-resolution climate model. *Journal of Climate*, *30*(5), 1629–1641. https://doi.org/10.1175/JCLI-D-16-0120.1

Zanowski, H., Hallberg, R., & Sarmiento, J. L. (2015). Abyssal ocean warming and salinification after Weddell polynyas in the GFDL CM2G coupled climate model. *Journal of Physical Oceanography*, *45*(11), 2755–2772. https://doi.org/10.1175/JPO-D-15-0109.1